TDA Progress Report 42-99 November 15, 1989

Parkes Radio Science System Design and Testing for Voyager Neptune Encounter

T. A. Rebold and J. F. Weese
Telecommunications Systems Section

The Radio Science System installed at Parkes, Australia for the Voyager Neptune encounter was specified to meet the same stringent requirements that were imposed upon the DSN Radio Science System. This article describes the system design and test methodology employed to meet these requirements at Parkes, and presents data showing the measured performance of the system. The results indicate that the system operates with a comfortable margin on the requirements. There was a minor problem with frequency-dependent spurious signals which could not be fixed before the encounter. Test results characterizing these spurious signals are included.

I. Introduction

In conjunction with efforts to upgrade the DSN in support of the Voyager Radio Science experiments at Neptune, a Radio Science receiving system was temporarily installed at the Commonwealth Scientific Industrial Research Organization (CSIRO) Radio Telescope located in Parkes, New South Wales. The primary motivation for the Parkes installation was to allow improved signal reception at X-band through the application of signal arraying techniques between the Parkes 64-m antenna and the Canberra Deep Space Communications Complex (CDSCC) 70-m antenna located some 300 km away.

This article presents an overview of the Radio Science System at Parkes. Section II covers the performance requirements imposed by the Voyager Neptune encounter, and is followed in Section III by a description of the design chosen to meet these requirements. The test methodology for verifying system performance is discussed in Section IV, with the results from tests performed in March 1989 presented in Section V.

The results in Section V show a system that is meeting its performance requirements to an outstanding degree. Both the long- and short-term frequency stability measurements show performance margins of about an order of magnitude better than the requirements. The only exceptions are the frequency-dependent spurious signals generated by an internal frequency synthesizer which is used to tune the carrier into a narrow bandwidth. This represents a subsystem problem that was identified at an early stage, but was not deemed significant enough to warrant a major subsystem change prior to encounter. In order to understand and characterize these spurious signals, however, a calibration test was run, and the results are also included in Section V.

Although this article presents a complete overview of the Parkes system, it supplements a previous article documenting the associated Radio Science Systems installed at CDSCC and at the Usuda, Japan station [1]. Interested readers will also find in this reference a description of the Radio Science experiments, an elaboration on the phenomenon of phase noise and how it degrades the performance of the Radio Science System, and a fuller account of the system test hardware and methodology.

II. System Performance Requirements

Spacecraft Radio Science is concerned primarily with two types of measurements: (1) occultation measurements in which the spacecraft signal passes through a planetary atmosphere, ionosphere, or ring system as it propagates to Earth, and (2) gravitation measurements in which the planet's gravity field perturbs the spacecraft trajectory and hence the downlink Doppler frequency [2]. Radio Science as performed at Parkes, however, is concerned only with the occultation measurements.

For these measurements, there are certain aspects of the spacecraft carrier, namely the fluctuations in its amplitude and phase, from which the properties of the planetary medium can be determined. The Radio Science System is required to record the spacecraft carrier with minimal degradation to these parameters. However, there are many noise processes in the system that may contribute toward their degradation. These include thermal noise, short-term phase noise, receiver-generated spurious signals, long-term phase drifts due to diurnal temperature changes, and gain instabilities.

Of these noise sources, the most critical are those relating to phase stability, both long- and short-term, including spurious signals. Although amplitude, or gain, instabilities are important, they typically exist at levels well below comparable levels of the phase instabilities. This is because any phase-noise components and line spectra spurious signals that enter the first local oscillator (LO) chain at a low frequency level, say 5 MHz, are severely exaggerated by the frequency multiplication performed to generate the X-band LO. This property does not apply to amplitude noise.

Long-term phase fluctuations on the order of 1000 sec in the receiver LOs can prevent the correlation of data between two receiving stations, which in turn reduces the effective signal-to-noise ratio (SNR) of the combined data. Short-term phase-noise processes generated in the receiver, on the other hand, corrupt the power spectrum of the received signal more directly by masking the phase fluctuations placed upon the carrier by the planetary media. Spurious signals generated within the receiver also corrupt the received signal spectrum in such a way as to interfere with the filtering that is performed when the data are processed.

Since the phase stability of the Radio Science System is important over such a wide range of time scales (from 1000 sec to 0.1 msec), the requirement for it is divided into two requirements over two different time scales. The long-term phase stability is specified from 1 to 1000 sec using the Allan variance parameter, which is a universally accepted measure of fractional frequency deviation [3, 4]. The Voyager Neptune requirement for the system Allan deviation is 6×10^{-13} for 1-sec integration times and 3×10^{-13} for 10- to 1000-sec integration times. The short-term phase stability is specified using $\mathcal{L}(f_m)$, the single-sideband spectral density of the phase noise at a carrier offset frequency of f_m, where f_m ranges from 1 Hz to 10 kHz. The required level of the single-sideband phase noise is -53 dBc/Hz at an f_m of 1 Hz, and -60 dBc/Hz from 10 Hz to 10 kHz.

The spurious signals mentioned previously refer to discrete sinusoidal components within the sideband spectrum which are generated when line currents from AC power supplies or other electromagnetic interference (EMI) sources modulate the LO signals. The Voyager Neptune requirement for the system spurious signals is the same level as the phase-noise requirement using a 1-Hz measurement bandwidth (although the spurious signals maintain a level independent of the measurement bandwidth): -53 dBc single-sideband at 1 Hz offset from the carrier, and -60 dBc from 10 Hz to 10 kHz.

III. System Configuration

Figure 1 shows a block diagram of the Radio Science System at Parkes. The antenna is a 64-m dish which gathers and focuses incoming signal flux density to a feed in the aerial cabin, a small room situated at the apex of the tripod structure built upon the dish. Inside the aerial cabin are two traveling-wave masers (TWMs) which can be configured to look at the sky or an ambient load termination. The noise-adding radiometer (NAR) injects its noise diodes immediately prior to the TWMs. Also in the aerial cabin are two RF-IF converters which convert the X-band received signal of 8415 MHz to a 315-MHz IF. Each TWM has its own dedicated RF-IF converter. Taken together, the two TWM and RF-IF channels constitute a primary and backup subsystem. Following conversion, the two IF outputs are sent down a cable run to the Parkes Canberra Telemetry Array (PCTA) van. Inside the van is a switching assembly that selects the prime or backup IF channel and sends it to both the telemetry receiver and the Radio Science Data Acquisition Subsystem (DAS).

The DAS contains dual parallel IF-VF converter channels and recording assemblies. Two channels are needed to prevent loss of data when the spacecraft switches between the coherent mode of transmission in which the downlink is phase-locked to the uplink, and the noncoherent mode in which the downlink is derived from the onboard Ultra-Stable Oscillator (USO). This is because a single-channel DAS is not able to continuously track the 5.4-MHz shift in received X-band carrier frequency that results from the mode change; it would have to be halted and restarted with a different frequency-tuning predict set. Thus with a dual-channel DAS, each of the two channels is assigned one of the modes and is preprogrammed to track the time-frequency profile of this mode. The two channels are run in parallel so that when a mode change occurs, the signal disappears from one channel and appears immediately on the other channel.

The basic channel in the DAS consists of a Radio Science IF-VF Converter (RIV) followed by a Mark III Occultation Data Assembly (ODA) that digitizes the video signal, tape records the signal, and controls the LO frequency in the RIV. The ODA is made up of a Mark III Narrow-Band Occultation Converter (NBOC), a Modcomp II computer with an IBM PS/2 computer to provide terminal input, and two Wanco tape drives for storing digitized data. For frequency tuning purposes, the Modcomp II computer accepts and stores predict sets of up to 42 points. The predict sets are entered through the PS/2 terminal. The local oscillator used in the RIV is tunable by the ODA computer so that the received spacecraft carrier containing Doppler shift can be kept within the 35-kHz VF-filter bandwidth. The LO mixer injection frequency is derived by frequency multiplying the output of the computer-controlled Dana synthesizer by a factor of seven in order to achieve the desired LO frequency range. The tuning capability is provided by the Programmed Oscillator Control Assembly (POCA), which takes frequency and ramp-rate commands from the Modcomp II computer and controls and monitors the Dana synthesizer accordingly.

The Parkes IF-VF converter is different from the type used in the DSCC Radio Science System in terms of how the bandwidth limiting is accomplished and how the adjacent sideband noise spectrum is rejected from folding over into the passband. The DSCC design uses a quartz-crystal bandpass filter with a center frequency that is offset from the final LO, while the Parkes configuration uses a single-sideband (SSB) mixer for converting the IF directly to VF. The SSB mixer passes the upper sideband, which contains the carrier, and rejects the lower sideband, which contains only noise. The LO for the SSB mixer is offset below the carrier by one-half of the desired video bandwidth. A VF lowpass filter (LPF) following the SSB mixer band limits its output so that the combination forms an equivalent 35-kHz bandpass-type filter, which acts as an anti-aliasing filter for the digital sampling process. A VF amplifier follows the LPF to drive the digitizer in the NBOC.

The video signal is monitored on a spectrum analyzer at a point just prior to its digitization. Also, an RMS voltmeter measures the level of the input signal to the analog-to-digital converters (ADCs) in the NBOC. During system precalibrations, the RIV attenuator is adjusted to achieve a video level, which is largely thermal noise power, of about 1 volt RMS in order to avoid saturating the ADCs.

After sampling the signal, the NBOC sends the digitized data to the Modcomp II for magnetic tape recording. The Modcomp II reads each byte immediately after it has been written to the tape and sends the data back to the NBOC. The NBOC then converts the digital samples back to an analog signal that can be monitored with a spectrum analyzer to verify that the desired data are being recorded to tape.

The Frequency and Timing Subsystem (FTS) at Parkes uses two hydrogen-maser frequency standards located in a temperature-stabilized room that is remote from the PCTA van for magnetic isolation purposes. The frequency standards provide 5-MHz references to the PCTA van, each sent through a quartz-crystal oscillator clean-up loop (CUL) to improve the phase noise at low signal offset frequencies near 1 Hz. The output of the prime CUL is distributed throughout the van using two HP5087 distribution amplifiers. The HP5087 amplifiers supply reference signals to all of the time-code generators (TCGs) in the van, which in turn provide timing signals to the ODA and telemetry computers.

The redundant receiver first local oscillators are derived from the 5-MHz CUL output. First, a $\times 20$ multiplier in the PCTA van multiplies the CUL output up to 100 MHz. Two 100-MHz outputs are sent via hardline coaxial cables to the aerial cabin. There the 100-MHz signals are further multiplied by a factor of 81 to provide the 8.1-GHz first LOs to the RF-IF downconverters.

IV. System Test Methodology

The system testing at Parkes was aided by the test methodology and hardware that had been developed for the CDSCC. Both of the instruments developed for Radio Science System stability testing—the test transmitter and the digital stability analyzer (DSA)—were designed to be transportable between the Canberra and Parkes facilities.

The block diagram of the Radio Science System at Parkes in Fig. 1 shows this test instrumentation. The methodology for Radio Science System stability testing involves injecting a highly stable RF test signal into the TWM input and measuring the stability of the test signal after it has been downconverted to video-frequency, digitized by the NBOC, and then reconstructed back to an analog waveform. This procedure is a direct means of measuring the amount of degradation the entire system imposes upon the received signal.

The RF test signal is generated by the portable test transmitter. The transmitter contains a phase-stable quartz-crystal oscillator for performing phase-noise measurements, and is phase-locked to an FTS 5-MHz reference for performing Allan variance measurements. To reliably measure the Radio Science System's performance, the transmitter was designed with performance requirements about an order of magnitude better than the Radio Science System requirements.

There are two places where the RF test signal can be injected into the system. The test transmitter is equipped with an RF horn so that the signal can be radiated into the antenna feed from a strategic point on the ground. However, the proximity to the antenna of most convenient locations on the ground tends to give rise to multipath effects which distort the test results. For all of the system tests described in Section V, the multipath problem is avoided by injecting the test signal into the system through a coupler at the TWM input.

In order to improve the system SNR, a 30-dB attenuator is inserted into the signal path immediately following the TWM. This allows injecting a 30-dB stronger signal into the TWM without saturating the following receiver subsystem. However, the resulting increase in SNR is only about 19 dB because the thermal noise of the receiving subsystem now becomes the dominant component of the system noise temperature.

For signal analysis, the digital stability analyzer accepts the system's video-frequency output either prior to or following digitization and processes it for phase noise and Allan variance information. The DSA is essentially a computer containing its own ADC for signal acquisition, as well as digital signal processing hardware and software to measure the power spectrum of a video test signal and decompose it into the quadrature component amplitude and phase spectra. The system phase-noise response can be read directly from the phase spectrum. For Allan variance tests, the DSA contains hardware which downconverts the video signal to 1 Hz. A time-interval counter samples the zero crossing of this 1-Hz signal and sends it to the DSA's computer for processing [1, 3, 4].

During the phase-noise test, the test transmitter is ideally configured to run on its internal oscillator so that there is no coherence between the system's reference frequency and the test signal. With this configuration the entire system performance is measured, including that of the hydrogen-maser frequency standard. On the other hand, for Allan variance testing the test transmitter must be phase-locked to the station FTS because the long-term stability of its quartz-crystal oscillator is inadequate for measuring system performance over long test periods. Because the transmitter is phase-locked to the station FTS, the FTS effects cancel out. Therefore, the stability of the FTS must be measured separately with the DSA by comparing the two similar hydrogen-type masers.

V. System Test Results

The testing of the Radio Science receiver at Parkes helped to uncover and remove many problems that were not apparent at the subsystem level. However, the results shown here include only typical performance curves taken after most of the problems had been removed. In addition, measurements taken with the NAR operating in encounter configuration are also presented. The last section summarizes a special calibration test made on the Dana LO synthesizers in the IF-VF converters. This test was performed to help characterize the behavior of certain frequency-dependent spurious signals that are generated by these synthesizers.

A. Allan Variance Test Results

Figure 2 shows the Allan variance results of the system measured with the DSA. These data were taken using the test transmitter, the prime 5-MHz CUL, the hydrogen maser, and the backup (channel 1) ×81 multiplier feeding into the prime (channel 2) RF-IF downconverter. The unusual ×81 configuration was implemented to bypass a malfunctioning unit. These results represent the system at its best performance. The Allan deviation at 1 sec is almost an order of magnitude below the 6.0E-13 specification. The only concern is the peak at about 1000 sec which represents a long-term drift in the system phase. The source of the drift was not determined with confidence, so it could be due to the test transmitter, system cable temperature effects, or the LO multiplier chain. In any event, the peak is still an order of magnitude better than the system specification.

B. Phase Noise and Power Spectrum Tests

Figure 3 shows the system phase-noise spectral density measured with the DSA. The hydrogen-maser frequency standard was used. The system configuration was not optimal since a ×81 frequency-multiplier unit that later proved to be defective was used, although it was not malfunctioning during this period. The frequency span of the plots is 200 Hz around the carrier and shows detail on a number of spurious signals. Of particular interest is a set at 1 Hz, approximately −59 dBc below the carrier. The source of these spurs was not determined; however, they were not present during the later testing period and do not show up in the final data (for example, see Fig. 4).

Note that the level of the discrete sinewave components in Figs. 3 through 7 is adjusted to correct for the resolution bandwidth of the spectrum measurement. A spectrum analyzer typically measures the level of the discrete components of a signal correctly, but the continuous, broadband components need to be scaled by one over the resolution bandwidth of the measurement to indicate spectral density in units of dBc/Hz. For Figs. 3 through 7, the normalization has already been applied to the vertical axis so that the broadband noise components can be read directly off the plots in units of dBc/Hz. However, the normalization of the vertical axis makes the discrete component levels incorrect, so an adjustment is made to indicate their correct levels in units of dBc. Stated simply, the spectrum plots are corrected to show what the spectrum would look like if it was measured with a resolution bandwidth of exactly 1 Hz, and both the discrete (after correction) and continuous components are read off these plots using the same vertical scale.

For Figs. 8 through 11, only the discrete components are of interest, so the vertical axis is not adjusted. The discrete components are read off as they are plotted in units of dBc without any need for adjustment. The broadband components are plotted in units of dBc per the resolution bandwidth of the measurement (0.38 Hz, 0.38 Hz, 2.4 Hz, and 2.4 Hz respectively).

The plot in Fig. 3 shows that neither the discrete noise components nor the broadband noise components violate the phase-noise specification. However, it should be noted that the test transmitter in this case is phase-locked to the station FTS 5-MHz reference, so that the effects of FTS have cancelled out.

In order to measure the performance of the entire Radio Science System, including the FTS standard, the above test was repeated ten days later with the system again running on the hydrogen-maser frequency standard but with the test transmitter free running on its internal quartz-crystal oscillator. The uncertainty in the output signal frequency from the test transmitter made the use of the digital stability analyzer impractical for making system measurements, so the HP3561 spectrum analyzer was used to measure the power spectrum. Since the power spectrum is the root-sum-square of the phase and amplitude spectra, a power spectrum which meets the phase noise requirement implies a phase-noise spectrum which also meets the requirement.

Figures 4, 5, 6, and 7 show the single-sideband power spectrum around the carrier over four different frequency spans: 20 Hz, 400 Hz, 2 kHz, and 20 kHz. The close-in single-sideband noise power at 1 Hz is seen in Fig. 4 to be −57.3 dBc/Hz. This compares well with previous measurements of the test transmitter which showed a single-sideband phase noise at X-band of −58 dBc/Hz. The level at 10 Hz is less than −65 dBc/Hz. From 100 Hz to 10 kHz, the noise is less than −75 dBc/Hz. The power line spurs are less than −60 dBc, while the Dana spurs at 2.85 kHz are −52 dBc.

Figure 5 shows two sets of spurious signals that are generated by the Modcomp II computers in the ODAs. For comparison, Fig. 6 shows the power spectrum taken with the Modcomp IIs turned off. One set of spurs shows up (in Fig. 5) at about 109 Hz and is generated by the prime ODA. The other set of spurs at about 57 Hz is generated by the backup ODA. Over time both spurs were seen to drift randomly in frequency by several hertz or so.

The source of these spurs was unknown until the ODAs were switched off. Further investigation by the personnel at Parkes revealed that the spurs were generated by clock signals internal to the ODAs, which were not phase-locked to the FTS and hence slightly off-frequency. The clock signals were phase-modulating the FTS 5-MHz reference at the beat note frequency between the sixth harmonics of the two timing signals. The interaction was made possible through a faulty hardline connector that coupled the ODA clock radiation into the FTS 5-MHz signal. Even though the resulting spurious phase modulations were quite low on the 5-MHz line, they were exaggerated to a level of −45 dBc by the frequency multiplication factor needed to generate the 8.1-GHz first LO. The replacement of the faulty connector reduced the power of the spurious signals to an acceptable level.

Figure 8 shows the close-in power spectrum of the 20-kHz VF carrier with 3.5-Hz and 10.5-Hz offset spurs present. This test was run with the NAR injecting a 50-K noise diode modulated at 20 Hz into the signal path before the low-noise amplifier (LNA) maser. Since the spurs are only 48 dB below the carrier, and there was no time to investigate and reduce the interaction, it was recommended that the 50-K noise diode not be used during the prime Radio Science data-gathering time periods. Fortunately, the 1-K noise diode, which is currently planned for use during the encounter, does not contribute any measurable effect above −65 dBc, as shown in Fig. 9. Note that the test configuration was run without the 30-dB attenuator after the maser that is normally installed during system testing to improve the test signal's SNR, so the noise floor with this 100-Hz span is only −67 dBc. This was necessary because the 30-dB attenuator in the front end changes the system noise floor and renders the NAR inoperable.

C. Dana Calibration Tapes

A series of calibration tapes was run at Parkes to characterize the spurious signals generated by the Dana synthesizers, which are used to provide the tuned local oscillator in the IF-VF converter. During the early phase of subsystem testing at JPL, these synthesizers had exhibited two types of spurious signals which violated specifications. The first type was induced by power supplies in the Dana chassis and nearby instruments which modulated the Dana's crystal oscillator at the power-line frequency via magnetic field coupling. These spurs were reduced by shielding the synthesizers from magnetic flux and moving their internal power supplies into a separate chassis. The second type are frequency-dependent modulations on the synthesizer output that are generated by the internal digital circuitry of the synthesizer. These spurs have been measured on the video carrier as high as about −52 dBc in some cases and may actually shift across the carrier signal as the Dana frequency changes. Unfortunately, they could not be removed from the device without a fundamental change in its design.

In order to characterize the expected behavior of these spurs during the encounter, predict sets were generated that stepped the POCA-controlled Dana across the important parts of the encounter frequency range. Energy level is examined to characterize the effect of a spur close to the carrier when the Dana frequency is changed. A total of three predict sets of 21 frequency steps each was constructed. One set was made to cover the one-way mode prior to the Neptune occultation, a second set was made for the two-way mode prior to occultation, and a third set was made to cover the one-way mode after the occultation. The frequency range of the predict sets is defined in Table 1. The actual frequency of each point can be determined by the equation:

$$F(i) = F\text{start} + \frac{i(F\text{stop} - F\text{start})}{20} \quad \text{for } i = 0 \text{ to } 20$$

where Fstart and Fstop are taken from Table 1.

The tapes were made by simulating the spacecraft signal with an HP8662 synthesizer injected into the IF input at the RIV. During recording, the HP8662 was stepped in frequency with an HP85 computer so that the resultant video remained at 20 kHz for each step. The duration of each step was about 18 sec, with 1 sec allowed for frequency changes between steps.

Both of the Danas were calibrated with the three predict sets for a total of six tapes. The tapes were analyzed on the JPL Radio Occultation Data Analysis (RODAN) computer. Some of the results are presented below.

In general, the Dana with NASA serial #106227 is superior to Dana #118430 because it has much fewer spurs. Figures 10 and 11 compare #106227 with #118430 at a Dana frequency of 45578013.78 Hz taken from the one-way pre-occultation predict set. The pair of spurs at about 1.5 kHz from the carrier is at −57 dBc. When the Dana frequency is in this neighborhood, the 1.5-kHz spurs drift at a rate equal to ten times the change in Dana frequency, so it is natural to assume that they will cross the carrier at about the same level. In other words, if the Dana frequency increases by 100 Hz, the spurs will move closer to the carrier by 1 kHz, or will be about 500 Hz away.

Not all of the spurs obey this 10-to-1 dependency upon the Dana frequency. Other plots not shown here reveal a 1-to-1 relationship, and in one case a relationship much higher than 10 to 1 was observed.

In order to calculate the real effect of the Dana spurs upon the system, one must consider the rate at which they will move during encounter. Since a moving spur spreads its power across a finite frequency range, its level at one discrete frequency point in a measured power spectrum will be much lower than that of a stationary spur with the same power level. How much lower depends upon the rate at which the spur moves.

For example, the spectra in Figs. 10 and 11 are obtained by averaging successive fast-Fourier transforms (FFTs) of the sampled video signal. The data were sampled at 80 kilosamples/sec. A total of 32768 data points is used for each FFT. This gives an FFT bin spacing of approximately 2.44 Hz, with a data acquisition time of 0.4096 sec for one buffer of data. If instead of being a fixed frequency, the LO had tracked the carrier at a rate of about 30 Hz/sec due to Doppler (about the highest rate predicted for the Neptune encounter), the carrier would remain steady at the video frequency, but the spurs would change frequency. During the time it took to acquire the data for one FFT, the LO would move by 12.288 Hz. The Dana frequency itself would only change by 1.75 Hz because of the $\times 7$ frequency multiplier placed after the Dana. If the spurs were moving at a rate ten times the Dana frequency change, they would have shifted by 17.5 Hz or about seven FFT bins. Assuming a uniform ramp rate, the signal power would be divided evenly among seven FFT bins instead of one, with each bin showing only about one-seventh the original power of the spur. The peak power in this smeared spur would then be 8.5 dB lower than if the spur had not been smeared. If, however, the spur obeyed a 1-to-1 dependency upon the Dana frequency, it would move only 1.75 Hz and would likely spend most of the time within a single FFT bin, so no reduction in level would be observed.

VI. Conclusions

This article has outlined the installation of the Radio Science System at the Parkes Radio Telescope in New South Wales, Australia. The Voyager Neptune encounter performance requirements and system design were discussed, as well as the techniques used to measure the performance of the system and the actual data taken on site during performance verification. The results shown in Section V indicate that in general the system is performing with a comfortable margin on the desired characteristics. The problem areas remaining in the system are listed below.

In the area of Allan variance performance, the system is operating at about an order of magnitude better than specification. The only concern lies in a long-term phase drift that makes the Allan deviation rise up to about 1E-14 at 1000 sec. This is not in violation of specification, but could be a problem if it gets any worse.

In the area of phase-noise performance, the system is also operating at a level better than specification. An initial problem with the ODA computers generating unwanted modulations on the first LO was corrected with the replacement of a faulty hardline connector. The only remaining violations are the discrete frequency components generated by the Dana synthesizers described in Section V, which were considered too minor to warrant a major subsystem change to remove them.

Finally, a problem is noted concerning which noise diode is used in the NAR. A 50-K noise diode generates interfering spurious signals that show up at 3.5 and 10.5 Hz on the carrier at video frequencies, at about −48 dB below the carrier. However, no spurs above −65 dBc are measured when the 1-K noise diode is used.

The system is considered adequate and ready to receive and record the Voyager spacecraft signal during the upcoming Neptune encounter. It meets the basic system requirements and contains the additional functional capability to receive the downlink signal during the abrupt frequency shifts associated with spacecraft mode changes without loss of any data.

Acknowledgments

The authors would like to acknowledge the collaboration and guidance provided by N. Ham throughout the duration of this project.

References

[1] N. C. Ham, T. A. Rebold, and J. F. Weese, "DSN Radio Science System Design and Testing for Voyager-Neptune Encounter," *TDA Progress Report 42-97*, vol. January–March 1987, Jet Propulsion Laboratory, Pasadena, California, pp. 252–284, May 15, 1989.

[2] G. L. Tyler, "Radio Propagation Experiments in the Outer Solar System with Voyager," *Proceedings of the IEEE*, vol. 75, no. 10, pp. 1404–1430, October 1987.

[3] D. W. Allan, "Time and Frequency (Time-Domain) Characterization, Estimation, and Prediction of Precision Clocks and Oscillators," *IEEE Trans. on Ultrasonics, Ferro-electrics and Frequency Control*, vol. UFFC-34, no. 6, November 1987.

[4] C. A. Greenhall, "A Method for Using a Time Interval Counter to Measure Frequency Stability," *TDA Progress Report 42-90*, vol. April–June 1987, Jet Propulsion Laboratory, Pasadena, California, pp. 149–156, August 15, 1987.

Table 1. Predict sets used for Dana calibration

Set type	X-band range (GHz)		POCA range (MHz)	
	*F*start	*F*stop	*F*start	*F*stop
One-way Pre-occultation	8.419059	8.419124	45.577085	45.586371
Two-way Pre-occultation	8.41365255	8.41371755	44.804735	44.814021
One-way Post-occultation	8.419340	8.419404	45.617228	45.626371

FOLDOUT FRAME 1.

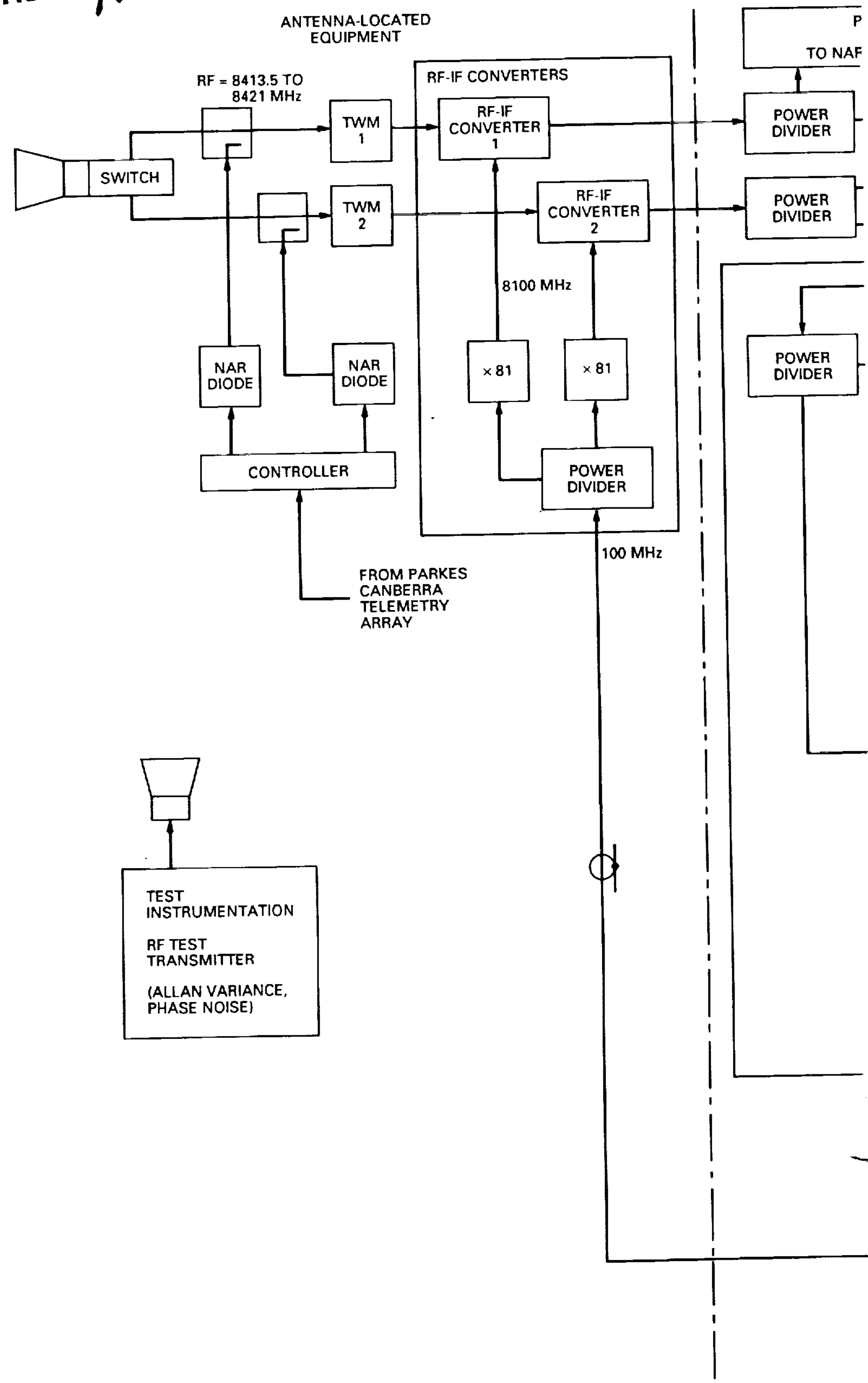

198.P

FOLDOUT FRAME 2 .

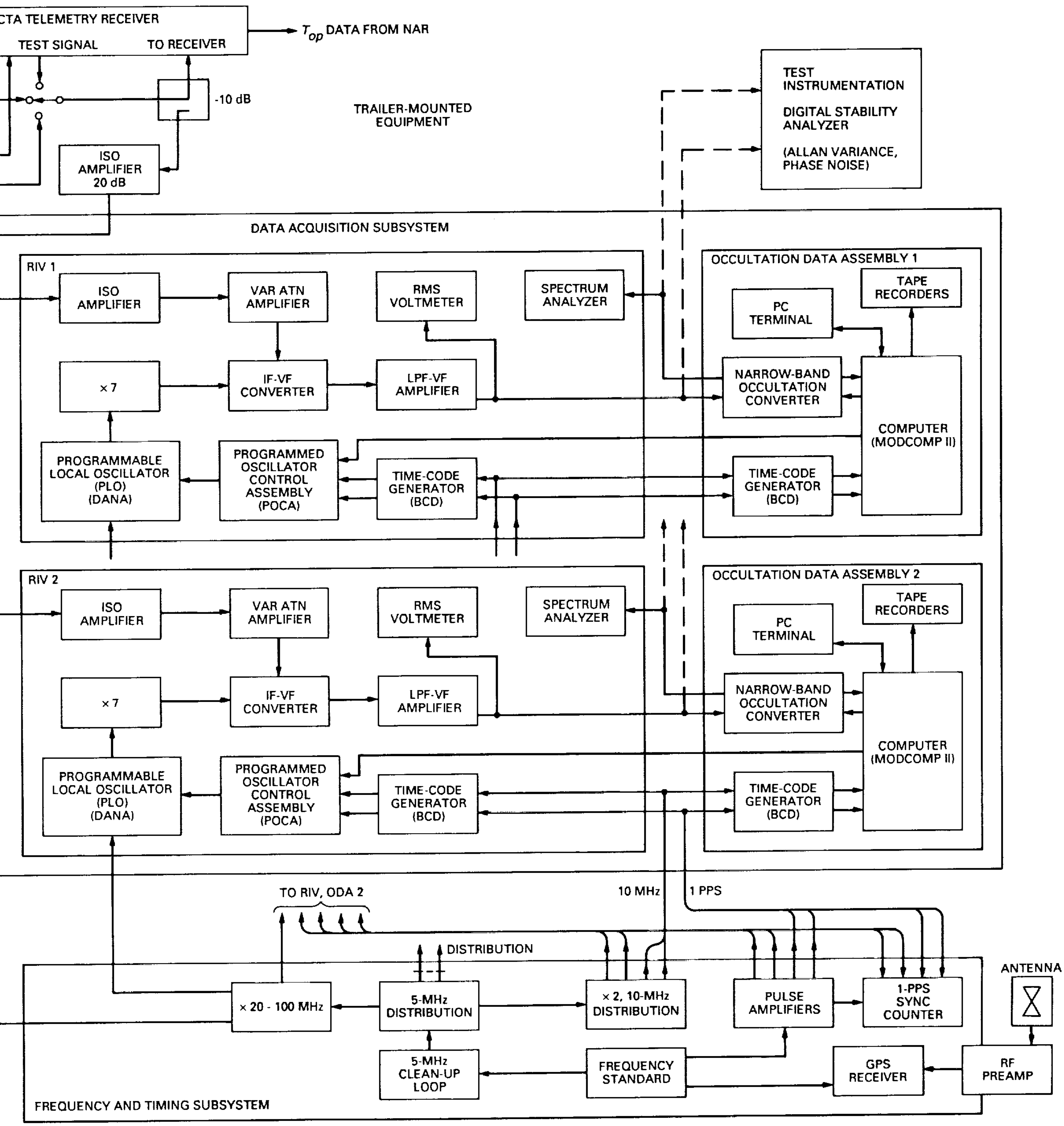

Fig. 1. Block diagram of the Parkes Radio Science System configuration.

ORIGINAL PAGE IS OF POOR QUALITY

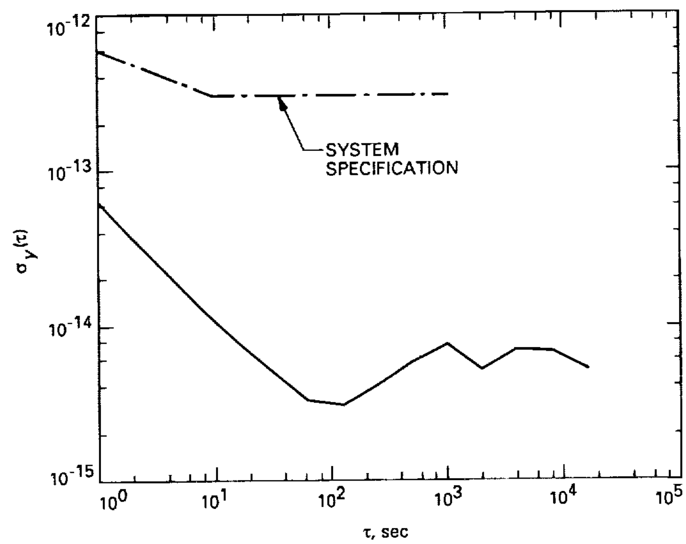

Fig. 2. Allan variance of the Parkes Radio Science System.

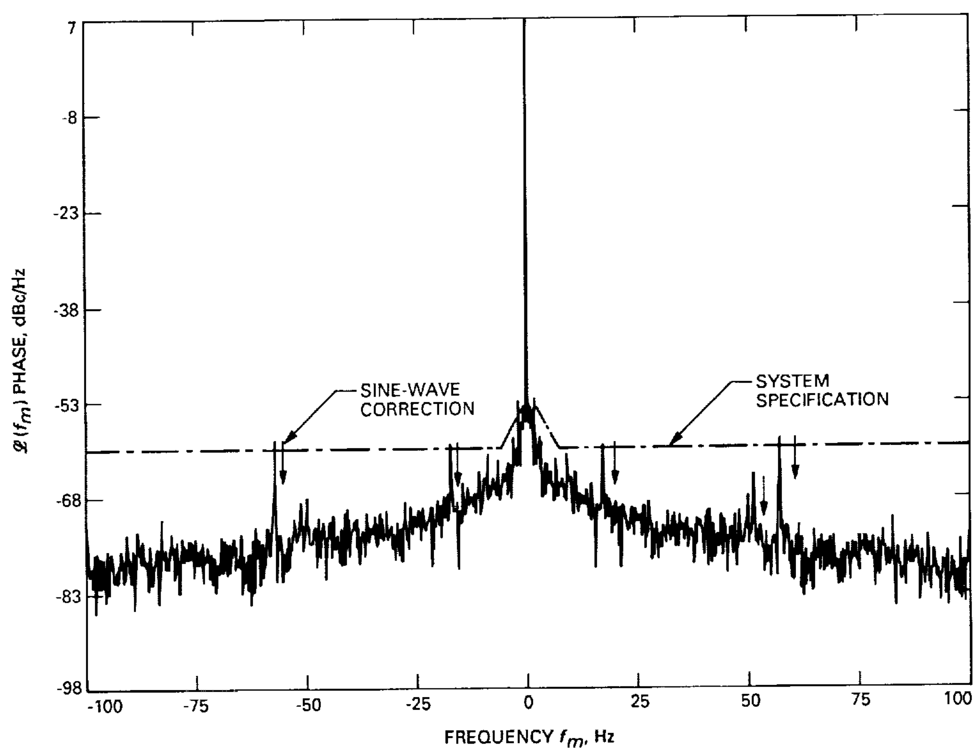

Fig. 3. Phase-noise spectral density of the Parkes Radio Science System, test transmitter phase-locked to FTS, −100 to +100 Hz (center frequency = 20 kHz).

PRECEDING PAGE BLANK NOT FILMED

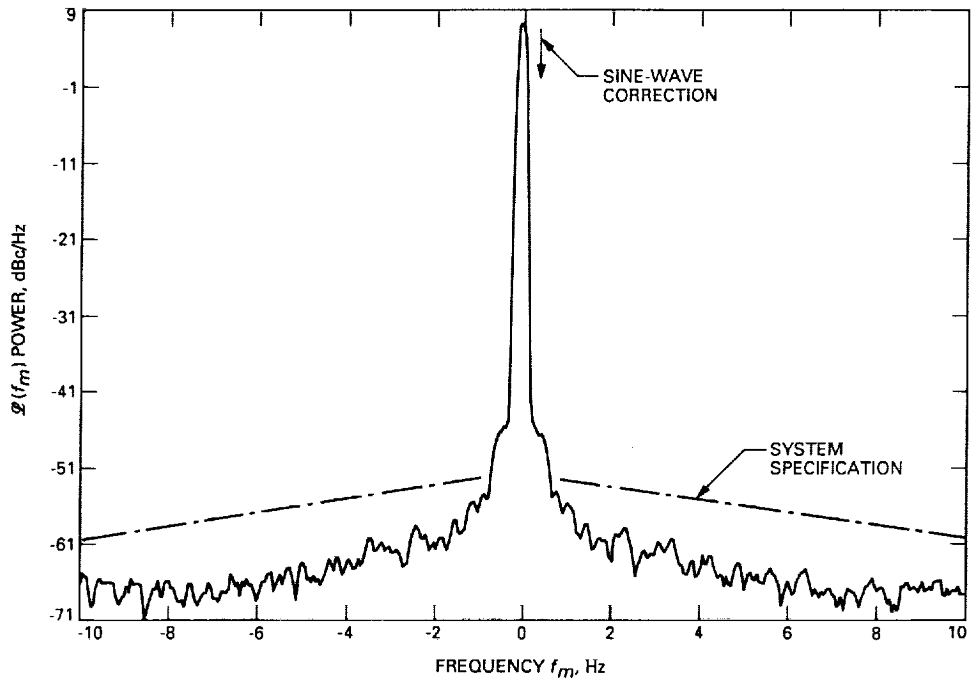

Fig. 4. Noise-power spectral density of the Radio Science System, test transmitter free-running, −10 to +10 Hz (center frequency = 19.95 kHz).

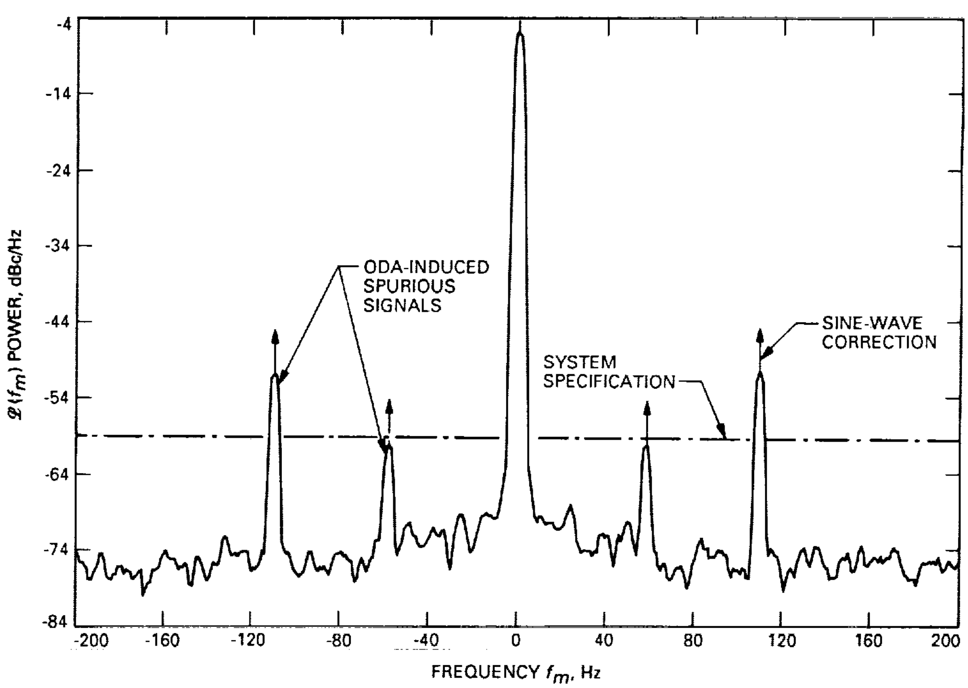

Fig. 5. System noise-power spectral density showing ODA-induced spurious signals, −200 to +200 Hz (center frequency = 19.95 kHz).

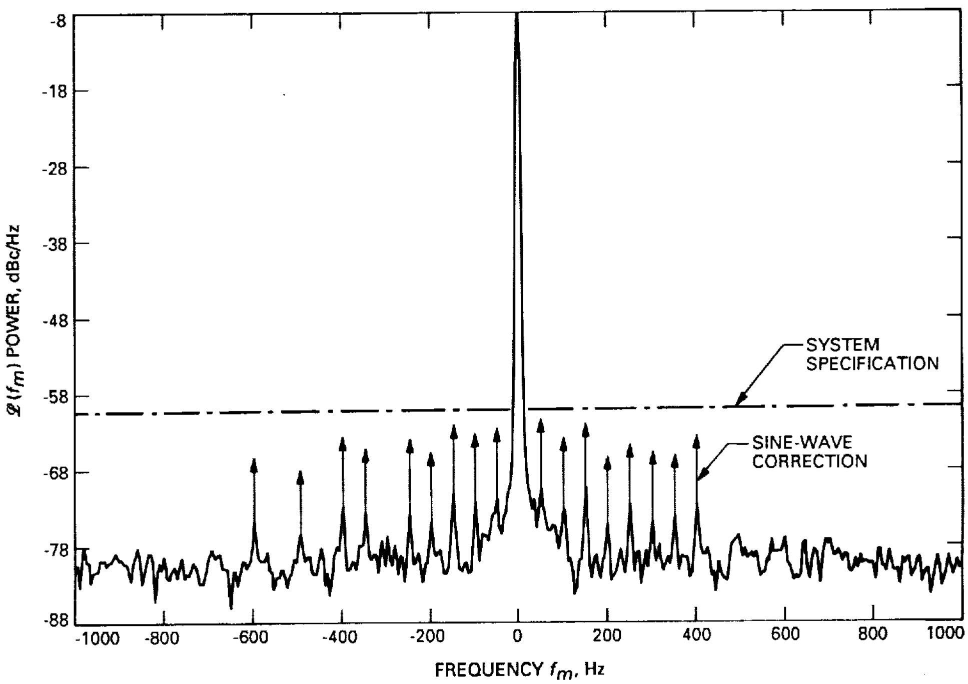

Fig. 6. System noise-power spectral density with ODAs turned off, −1000 to +1000 Hz (center frequency = 19.95 kHz).

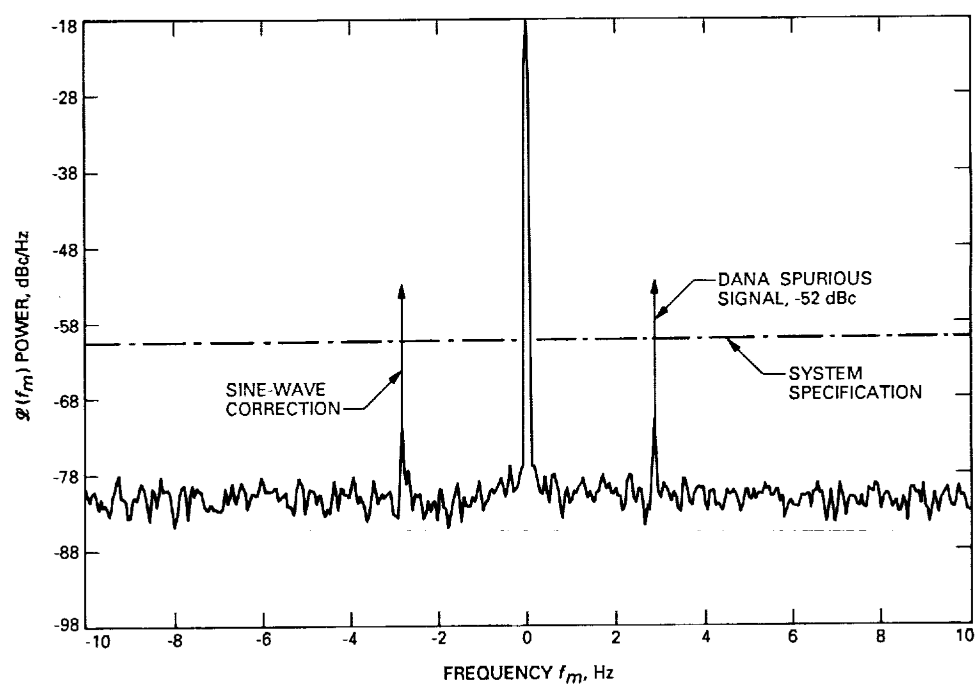

Fig. 7. System noise-power spectral density showing Dana spurious signals, −10 to +10 kHz (center frequency = 19.95 kHz).

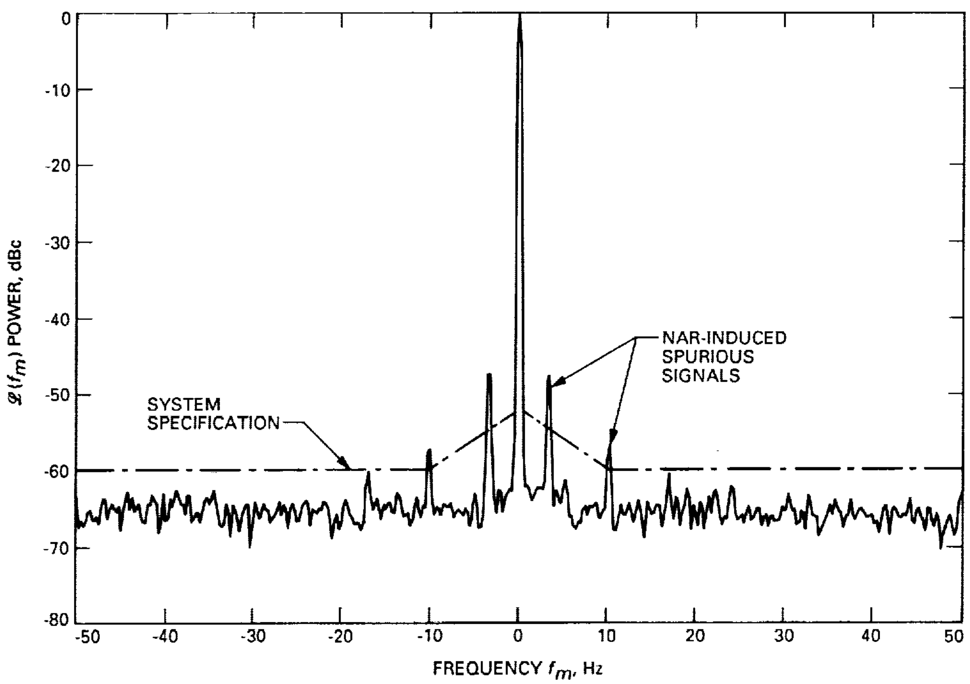

Fig. 8. System power spectrum showing spurious signals, NAR operating with 50-K noise diode.

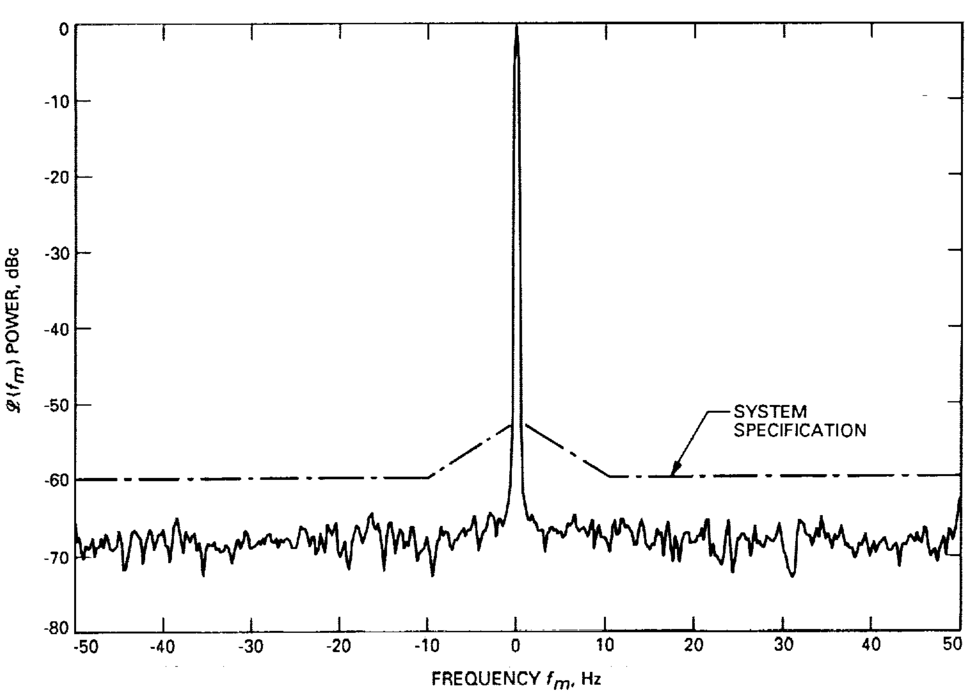

Fig. 9. System power spectrum showing no spurious signals, NAR operating with 1-K noise diode.

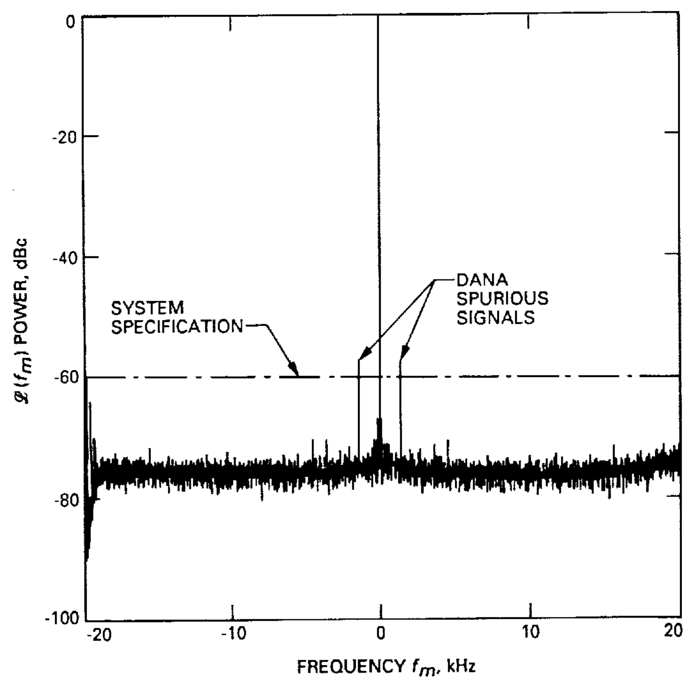

Fig. 10. Power spectrum showing Dana #106227-generated spurious signals, Dana frequency = 45.578013 MHz. Plot computed by JPL RODAN computer from tape-recorded samples.

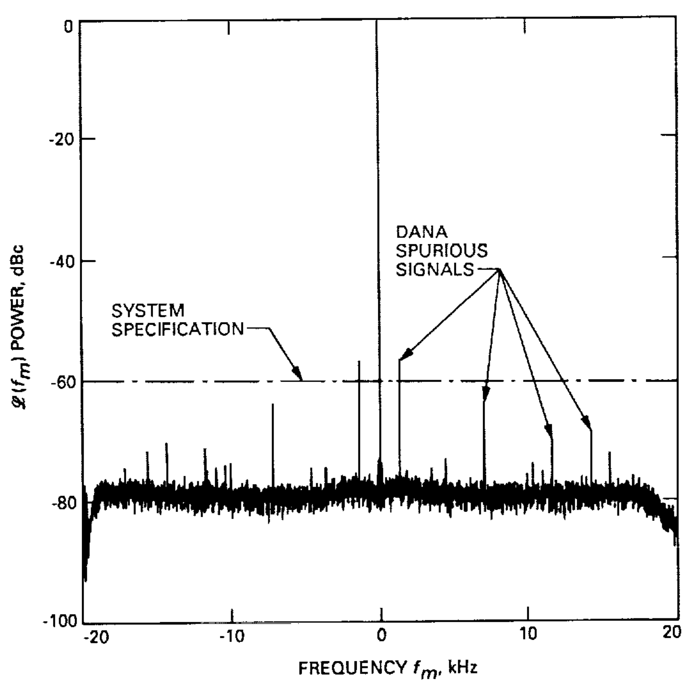

Fig. 11. Power spectrum showing Dana #118430-generated spurious signals, Dana frequency = 45.578013 MHz. Plot computed by JPL RODAN computer from tape-recorded samples.